ISSN 1674-1056
http://cpb.iphy.ac.cn
http://iopscience.iop.org/cpb
中国物理 B
Chinese Physics
中国物理
Chinese Physics B

Adsorption behavior of triphenylene on Ru(0001) investigated by scanning tunneling microscopy

Li-Wei Jing(井立威), Jun-Jie Song(宋俊杰), Yu-Xi Zhang(张羽溪), Qiao-Yue Chen(陈乔悦), Kai-Kai Huang(黄凯凯), Han-Jie Zhang(张寒洁), Pi-Mo He(何丕模)

Citation: Chin. Phys. B . 2019, 28(7): 076801. **doi:** 10.1088/1674-1056/28/7/076801
Journal homepage: http://cpb.iphy.ac.cn; http://iopscience.iop.org/cpb

What follows is a list of articles you may be interested in

Epitaxial fabrication of two-dimensional $TiTe_2$ monolayer on Au(111) substrate with Te as buffer layer

Zhipeng Song(宋志朋), Bao Lei(雷宝), Yun Cao(曹云), Jing Qi(戚竞), Hao Peng(彭浩), Qin Wang(汪琴), Li Huang(黄立), Hongliang Lu(路红亮), Xiao Lin(林晓), Ye-Liang Wang(王业亮), Shixuan Du(杜世萱), Hong-Jun Gao(高鸿钧)

Chin. Phys. B . 2019, 28(5): 056801. **doi:** 10.1088/1674-1056/28/5/056801

Image potential states mediated STM imaging of cobalt phthalocyanine on NaCl/Cu(100)

Qinmin Guo(郭秦敏), Zhihui Qin(秦志辉), Min Huang(黄敏), Vladimir N. Mantsevich , Gengyu Cao(曹更玉)

Chin. Phys. B . 2016, 25(3): 036801. **doi:** 10.1088/1674-1056/25/3/036801

Performance improvement in polymeric thin film transistors using chemically modified both silver bottom contacts and dielectric surfaces

Xie Ying-Tao, Ouyang Shi-Hong, Wang Dong-Ping, Zhu Da-Long, Xu Xin, Tan Te, Fong Hon-Hang

Chin. Phys. B . 2015, 24(9): 096803. **doi:** 10.1088/1674-1056/24/9/096803

Scanning tunneling microscopy study of molecular growth structures of $Gd@C_{82}$ on Cu(111)

Chen Jian, Qin Zhi-Hui, Pan Jin-Bo, Lu Shuang-Zan, Du Shi-Xuan, Gao Hong-Jun, Cao Geng-Yu

Chin. Phys. B . 2013, 22(7): 076802. **doi:** 10.1088/1674-1056/22/7/076802

Kinetic Monte Carlo simulations of optimization of self-assembly quantum rings growth strategy based on substrate engineering

Liu Jian-Tao, Feng Hao, Yu Zhong-Yuan, Liu Yu-Min, Shi Qiang, Song Xin, Zhang Wen, Peng Yi-Wei

Chin. Phys. B . 2013, 22(4): 046801. **doi:** 10.1088/1674-1056/22/4/046801

Adsorption behavior of triphenylene on Ru(0001) investigated by scanning tunneling microscopy*

Li-Wei Jing(井立威)[1], Jun-Jie Song(宋俊杰)[3], Yu-Xi Zhang(张羽溪)[4], Qiao-Yue Chen(陈乔悦)[1], Kai-Kai Huang(黄凯凯)[1], Han-Jie Zhang(张寒洁)[1,†], and Pi-Mo He(何丕模)[1,2,‡]

[1] *Zhejiang Province Key Laboratory of Quantum Technology and Device, Department of Physics, Zhejiang University, Hangzhou* 310027, *China*
[2] *Collaborative Innovation Center of Advanced Microstructure, Nanjing University, Nanjing* 210093, *China*
[3] *School of Information Science and Engineering, Ningbo Institute of Technology, Zhejiang University, Ningbo* 315100, *China*
[4] *Department of Fundamental and Social Science, Zhejiang University of Water Resources and Electric Power, Hangzhou* 310018, *China*

(Received 6 April 2019; revised manuscript received 3 May 2019; published online 12 June 2019)

As a representative of small aromatic molecules, triphenylene (TP) has markedly high carrier mobility and is an ideal precursor for building graphene nanostructures. We mainly investigated the adsorption behavior of TP molecules on Ru(0001) by using scanning tunneling microscopy (STM). In submonolayer regime, TP molecules are randomly dispersed on Ru(0001) and the TP overlayer can be thoroughly dehydrogenated and converted into graphene islands at 700 K. Due to weak interaction between TP molecules and graphene, the grooves formed among graphene islands have confinement effect on TP molecules. TP adopts a flat-lying adsorption mode and has two adsorption configurations with the 3-fold molecular axis aligned almost parallel or antiparallel to the $[1\bar{1}00]$ direction of the substrate. At TP coverages of 0.6 monolayer (ML) and 0.8 ML, the orientational distributions of the two adsorption configurations are equal. At about 1.0 ML, we find the coexistence of locally ordered and disordered phases. The ordered phase includes two sets of different superstructures with the symmetries of $(\sqrt{19}\times\sqrt{19})R23.41^\circ$ and $p(4\times4)$, respectively. The adsorption behavior of TP on Ru(0001) can be attributed to the delicate balance between molecule–substrate and molecule–molecule interactions.

Keywords: self-assembly, ordered superstructure, scanning tunneling microscopy

PACS: 68.43.Fg, 68.37.Ef, 68.43.–h **DOI:** 10.1088/1674-1056/28/7/076801

1. Introduction

The rapid development of molecular electronics took off in tandem with the rise of the nanoscience era in the past decades.[1–4] Bottom-up self-assembly of molecular building blocks at interfaces has been an extremely powerful method for fabricating highly functional nanostructures and nanoscale electronic devices with tailored properties.[5–9] The versatility of organic molecular materials can be preserved by some symmetry requirements in molecular assemblies. Microscopic ordering significantly enhances the high performance of organic electronic and optoelectronic devices, such as organic field-effect transistors (OFETs), organic light-emitting diodes (OLEDs), or photovoltaic solar cells.[10] To date, molecular assemblies on novel two-dimensional (2D) materials,[11,12] topological insulators,[13] semiconductors,[14] and metals[15–18] have sprung up. However, molecular assemblies on surfaces are not necessarily well-ordered. Manganese phthalocyanine on Bi_2Te_3 shows poor ordering, cytosine on Au(111) exhibits a random pore network, and the second layer of diF-TES-ADA is disordered despite ordering in the first layer.[6] Disorder at or near metal–organic interfaces can also play an essential role in raising the efficiency of charge injection.[19] So it is fundamentally important to have a comprehensive understanding of adsorption behaviors of molecules at interfaces and further improve the organic/substrate device performance. Generally, molecular self-assembly on the solid surface is governed by the delicate balance of intermolecular and molecule–substrate interactions. The driving mechanism of molecular self-assembly largely comes from different non-covalent intermolecular forces, such as hydrogen bonding,[5,20] π–π stacking,[21,22] dipolar,[23] electrostatic,[24] van der Waals,[25] and metal–ligand[26] interactions. Nevertheless, it is still a big challenge to precisely control and engineer desired architectures in reality, which stems from the complex interactions between adsorbates and substrates, coupling with the molecular geometry and intricate molecular deposition processes.

Polycyclic aromatic hydrocarbons with unique electronic and optoelectronic properties have aroused widespread interest. Functionalization of surfaces modified by aromatic molecules which have very high carrier mobility on single crystals is the paramount approach towards novel materials. Triphenylene (TP) is among aromatic molecules with π-conjugated system and can behave as both electron acceptors[27] and donors.[28] For example, TP has a comple-

*Project supported by the National Key Research and Development Program of China (Grant No. 2017YFB0503100) and the National Natural Science Foundation of China (Grant No. 11790313).

†Corresponding author. E-mail: zhj_fox@zju.edu.cn
‡Corresponding author. E-mail: phypmhe@zju.edu.cn

© 2019 Chinese Physical Society and IOP Publishing Ltd

mentary electronic density with trinitrotoluene (TNT) in electronic characteristics,[29] forming a donor–acceptor complex, which facilitates the molecular recognition of TP to TNT.[30] Because of the extended π-system of TP, it can be a precursor to fabricate graphene-like materials, such as graphene nanoribbons or nanographenes. In addition, TP can act as the scaffold for building new molecular materials to form self-assembly patterns[31,32] and liquid crystals.[33–35] However, studies on TP adsorbed on metal substrates have rarely been reported.

The ordering of the molecular orientation is affected by various factors. The key to steering adsorption configurations is the control over the strength of the molecule–metal interaction and its spatial variation. Great efforts have been devoted to investigations of molecules assembling into diverse superstructures by varying the substrates, where different electronic structures of substrates may lead to a series of rich and fascinating phenomena. For instance, anthraquinone (AQ) molecules on Au(111)[6] form a disordered pore network in contrast with a highly ordered regular giant honeycomb pore network observed on Cu(111).[36] Ru is a prototype transition metal with unoccupied d-shell, which has stronger surface reactivity than noble metals, such as Au(111), Ag(111), and Cu(111). Epitaxial graphene on Ru(0001) presents a molecular adsorption energy landscape with substantial periodic variation due to strong interaction of π–d electrons. So high surface activity aids in capturing small molecules from desorption and promotes the conversion into graphene at lower temperature.

The organic molecules with several aromatic groups have been in the spotlight in molecular self-assembly due to their ubiquitous π interactions making a strong contribution to their structure and stability. The structures and morphologies of the molecules on different substrates determine the charge injection and charge transport. To better understand the microscopic underpinnings of such molecules adsorbed on active metals and achieve efficient charge transport at interfaces, we here investigated the adsorption behavior of TP on Ru(0001) by means of scanning tunneling microscopy (STM) at room temperature. We firstly present the conversion stage of TP molecules into graphene nanostructures at low coverage and then analyze the adsorption configurations of TP on Ru(0001) at different coverages. Finally, TP molecular self-assembly superstructures are exhaustively discussed.

2. Experimental methods

The experiments were performed in a multi-functional ultrahigh-vacuum (HUV) VT-SPM system (Omicron Instruments for Surface Science) with a base pressure better than 2×10^{-10} mbar. The system was described in detail elsewhere.[37] In brief, it consists of a fast entry, a preparation chamber, an analysis chamber, and a scanning tunneling microscopy (STM) chamber. The system is equipped with an electron beam heating setup, a low-energy electron diffraction (LEED) attachment, an x-ray photoemission spectrometer, etc.

The Ru(0001) substrate was *in situ* cleaned by several cycles of argon ion sputtering (1500 eV$\times$1 h) and subsequent annealing at 1273 K. The substrate surface then was confirmed to be atomically clean and flat by LEED and STM measurements before molecular deposition. The commercial triphenylene powder (98% purity) purchased from J&K Scientific Company was loaded in a homemade Ta boat and thoroughly degassed overnight in the fast-entry chamber. The Ta boat was also used to sublimate TP molecules onto the Ru(0001) substrate by direct current heating while keeping the substrate at room temperature. The deposition dosage was carefully controlled by the deposition rate and time. All the STM measurements were conducted in constant current mode using an electrochemically etched tungsten tip at room temperature and the given bias voltages were applied to the sample with respect to the tip. The experimental STM images were processed within WSxM software.[38]

3. Results and discussion

Figure 1(a) displays the TP molecular ball-and-stick model. This planar molecule consists of four fused benzene rings with C_{3h} symmetry. As shown in Fig. 1(b), at the TP coverage of $\sim$0.3 monolayer (ML), molecules were randomly dispersed on the Ru(0001) surface. On the step edges, the image is blurry along the scanning direction. No ordered structures spontaneously formed. Subsequent annealing of the sample was proceeded at 400 K and 500 K respectively. Figure 1(c) is the overview STM image collected on the sample after annealing at 500 K, in which many bright spots came up. Figure 1(d) shows the close-up of the square region outlined in Fig. 1(c). A few protruding bright spots distributed randomly on the Ru(0001) surface. Based on the apparent height about 196 pm and the lateral size about 1.575 nm of the protruding spot measured by the line profile in Fig. 1(e), it is speculated that the bright spots are carbon clusters.[39,40] The dark protrusions with the size measured to be about 0.8 nm in length and $\sim$0.6 nm in width with STM, which is comparable with the dimension of individual TP molecule, should be individual TP molecules. The distorted or non-triangular shape of the dark protrusion (individual TP molecule) should arise from the STM tip scanning at room temperature, since that TP overlayer at low coverage is not stable, and TP molecules are mobile. After further annealing the sample at 600 K, a small amount of graphitized flakes came into being and notably, they prefer to stay at the step edges, as shown in Fig. 1(f).

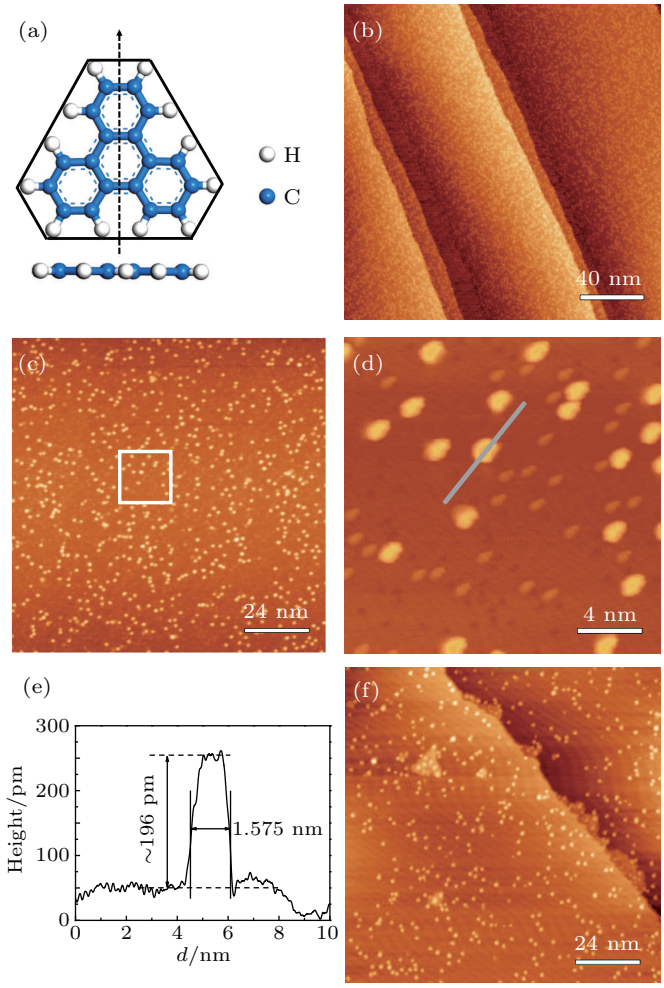


Fig. 1. (a) Schematic structural model of TP molecule (top view and side view) and one of the 3-fold axes is sketched as a dashed arrow. (b) Large-scale STM image for ∼ 0.3 ML of TP molecules on Ru(0001) (200 nm ×200 nm, $V_{tip} = -0.743$ V, $I = 0.915$ nA). (c) Overview STM image of intermediate products after annealing the sample at 500 K (120 nm×120 nm, $V_{tip} = -0.215$ V, $I = 0.915$ nA). (d) The close-up of the region outlined by the white square frame showing a few protruding bright spots without regular shapes in (c) (20 nm×20 nm, $V_{tip} = -0.215$ V, $I = 0.915$ nA). (e) Line profile along the gray line in (d), and (f) STM image of the graphitized nanoflakes formed after annealing ∼ 0.3 ML of TP molecules on Ru(0001) at 600 K (120 nm×120 nm, $V_{tip} = -0.203$ V, $I = 0.915$ nA).

Figure 2(a) demonstrates a large-scale STM image of ∼ 1.0 ML of TP molecules on the clean Ru(0001) surface, which is obviously a disordered structure. The molecules can be dehydrogenated and completely converted into graphene at 700 K (Fig. 2(b)). The conversion of graphene is demonstrated by formation of the Moiré patterns (the unit cell is sketched by a rhombus in Fig. 2(c)) due to the mismatch between the graphene layer and Ru(0001), and the Moiré superstructure has a periodicity of about 30 Å and a large height corrugation of about 1.5 Å.[41,42] In the present case, the Moiré patterns have a vertical corrugation of ∼ 1.2 Å and a lateral periodicity of ∼ 30 Å. The graphitization temperature of TP is fairly low compared to ethylene at ∼ 1000 K[43] on the Ru(0001) surface. So TP can be an ideal precursor to synthesize graphene nanostructures at low cost. It is interesting that there are a higher density of TP molecules in the grooves formed by a number of graphene islands and the step edges after further deposition of TP molecules onto the substrate, as shown in Fig. 2(c). During the whole scanning, we did not observe any molecule on the corrugated graphene/Ru(0001) at room temperature, suggesting an extremely weak interaction between TP and graphene. Therefore, graphene islands can act as the natural barrier to constrain the lateral movement of TP on the substrate. Figure 2(d) shows a typical STM image of 0.6 ML of TP molecules on the substrate. Upon adsorption on Ru(0001), the TP molecule remains intact and presents a triangular shape. Those molecules have two adsorption configurations with the 3-fold molecular axis (as shown in Fig. 1(a)) nearly going along either $[1\bar{1}00]$ or $[\bar{1}100]$ direction (also see Fig. 3), marked by red and green circles. The average size of the TP molecules is 1.0 ± 0.1 nm, which was carefully measured from the STM images of Figs. 3(c) and 3(d), in good agreement with the dimensions of TP. Together with the uniform brightness of TP on Ru(0001), we conclude that TP molecules are planarly adsorbed on the surface. It is widely accepted that the adsorption configurations of aromatic molecules are parallel to metal surfaces. The flat adsorption on the Ru(0001) surface can maximize overlap between the electronic structure of the substrate and the π-orbitals of the molecules which are involved in the bonding. For instance, p-terphenyl and 1,3,5-triphenylbenzene molecules even though not planar, their benzene ring backbones still tend to be parallel to the Ru(0001) surface from the pristine twisted structures.[44,45]

The observed two molecular axial orientations are mirror-symmetric to each other, which corresponds to a 60° rotation from each other. The array orientation of TP is largely dominated by the Ru(0001) surface. DFT simulation suggested TP on the Pt(111) surface has a preference for a hollow site.[46] Experimental results also showed that TP dominantly takes up the face-centered cubic (fcc) site and then occupies the hexagonal close-packed (hcp) site on the reconstructed Au(111) substrate.[47] It is proposed that the mutual coupling of the 3-fold symmetries of TP molecule and the substrate jointly requires TP occupying a 3-fold site of Ru(0001). Thus, the smallest energy-equivalent rotation is by 60°, equaling a reflection of TP.

Figure 2(e) shows 0.8 ML of TP molecules on the vacant area of Ru(0001) surface. The molecules irregularly pack into a disordered structure. At such high coverage, molecules neither aggregate into islands nor self-assemble into a long-range ordered structure spontaneously at room temperature. This suggests a stronger interaction between TP and Ru(0001), which is consistent with the previous conclusion that interaction between benzene π systems and transition metal surfaces results in the formation of stable chemical bonds.[48] Whereas, we also observed some fuzzy and seriously distorted molecular images along the fast scan direction (here from right to

left), which is the consequence of the lateral mobility of TP molecules on the substrate under the great influence of the tip during the scanning at room temperature. Besides, TP molecules tend to be far away from each other and try to take up more space. Schirmeisen *et al.*[47] also reported that the average distance of two closest neighboring TP molecules on Au(111) decreases with increasing coverage. The repulsive (weak) molecule–molecule interaction should be responsible for this adsorption behavior because a concentration of negative charges distribute in the TP molecular central region, leaving the rim positively charged[28] due to its flat-lying geometry on the substrate.

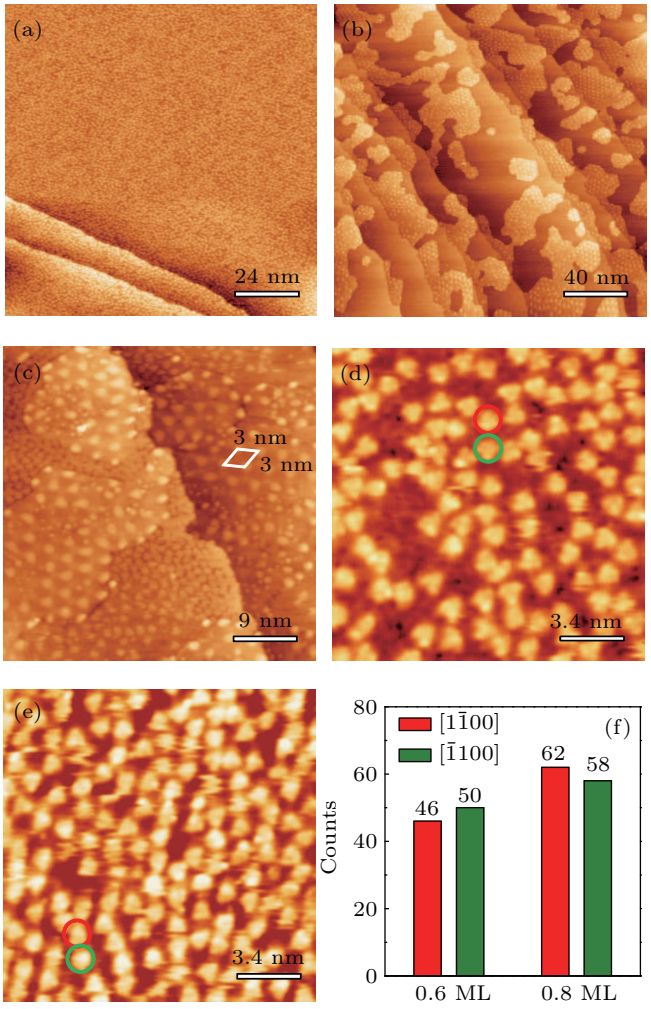


Fig. 2. (a) Large-scale STM image of $\sim$ 1.0 ML of TP overlayer on the bare Ru(0001) surface (120 nm×120 nm, $V_{\rm tip} = -0.224$ V, $I = 0.152$ nA). (b) STM image of graphene islands on Ru(0001) with typical Moiré patterns after annealing the sample at 700 K (200 nm ×200 nm, $V_{\rm tip} = -0.156$ V, $I = 0.309$ nA). (c) STM image for further deposition of TP molecules onto the substrate, showing partially high coverage of TP on the bare Ru(0001) surface constrained by a few graphene islands (the Moiré unit cell is sketched by a rhombus) and the step edges (45 nm×45 nm, $V_{\rm tip} = -0.086$ V, $I = 0.617$ nA). (d) STM image of 0.6 ML of TP molecules on Ru(0001) with two molecular orientations identified, indicated by red and green circles (they also apply to (e)) (17 nm×17 nm, $V_{\rm tip} = -0.073$ V, $I = 0.071$ nA). (e) STM image of 0.8 ML of TP molecules on Ru(0001) (17 nm×17 nm, $V_{\rm tip} = -0.358$ V, $I = 0.114$ nA). (f) The histogram counts of molecules corresponding to two molecular orientations at TP coverages of 0.6 ML and 0.8 ML.

The histogram in Fig. 2(f) demonstrates the number of TP molecules in two molecular orientations, which was counted from the STM images shown in Figs. 2(d) and 2(e). Within our statistics, a few molecules with severe distortion that cannot be identified with the configurations were removed. For TP coverages of 0.6 ML and 0.8 ML, each orientation contains almost the same number of molecules, which points out the equivalency of the two adsorption configurations. The equal orientational distribution is reasonable since both the TP molecule and the substrate have 3-fold symmetries and those two molecular orientations have an intersection angle of 60° between the 3-fold molecular axes. Similar experimental results were also observed for the TP overlayer on the reconstructed Au(111) surface at coverages of 0.4 ML and 0.7 ML.[47] Those results clearly indicate a dominant effect of the molecule–substrate interaction on the organic self-assembly.

Upon formation of graphene islands on Ru(0001), TP molecules were further deposited onto the substrate. Figure 3(a) is an overview STM image for TP molecules on the bare Ru(0001) with a coverage up to 1.0 ML. A vague view of relatively sparse molecular distribution and disordered structure is accessible on the wide terraces of the substrate. Interestingly, going along the narrow terrace which is surrounded with a few graphene islands, TP molecules self-assembled into small close-packed domains, outlined by white dashed contours. Figure 3(b) shows two coexisting ordered superstructures and the enlarged STM images in Figs. 3(c) and 3(d) display the structural details of two close-packed domains with TP imaged as triangles clearly. The protruding brightness of TP molecules is credited to the conjugated π-electron systems of TP making great contributions to the STM images.[49,50] As mentioned above, TP adopts two adsorption configurations. Apparently, each domain has a definite molecular orientation. For one close-packed domain shown in Fig. 3(c), the 3-fold molecular axis is almost along [$\bar{1}$100] direction but there is a small rotational angle of about 5° between the molecular axis and [$\bar{1}$100] direction. The unit cell is highlighted by the black rhombus. Based on the STM images, the lattice constants were measured to be $a_1 = b_1 = 1.2 \pm 0.1$ nm and $\alpha = 60° \pm 2°$. The proposed superstructure has a $(\sqrt{19} \times \sqrt{19})R23.41°$ symmetry. The corresponding schematic model is shown in Fig. 3(e), where the unit cell of the superstructure has the lattice constants of $a_1 = b_1 = 1.18$ nm and $\alpha = 60°$. For the other close-packed domain shown in Fig. 3(d), the molecular axis is almost aligned with [1$\bar{1}$00] with about a 5° rotational angle with respect to the [1$\bar{1}$00] direction. The unit cell is also indicated by the black rhombus with the lattice constants of $a_2 = b_2 = 1.1 \pm 0.1$ nm and $\beta = 60° \pm 2°$, where the basis vectors $\boldsymbol{a}_2$ and $\boldsymbol{b}_2$ are along [2$\bar{1}\bar{1}$0] and [1$\bar{2}$10] directions, respectively. The proposed superstructure has a $p(4 \times 4)$ symmetry and the corresponding structural model is displayed in Fig. 3(f), where $a_2 = b_2 = 1.08$ nm and $\beta = 60°$. The av-

erage areas of unit cells for those two superstructures are 1.21 nm^2 and 1.01 nm^2, respectively and each unit cell contains one molecule, which means the TP molecule in the former superstructure has larger space occupancy. In contrast, the close-packed structure of TP adsorbed on Au(111) has a $(\sqrt{13}\times\sqrt{13})R13.9^\circ$ symmetry.[47] Different superstructures of those two adsorption systems can be ascribed to different lattice constants of Ru(0001) ($d_{\mathrm{Ru-Ru}} = 2.706$ Å) and Au(111) ($d_{\mathrm{Au-Au}} = 2.880$ Å) and their distinct electronic structures.

The molecule–substrate and molecule–molecule interactions both play an essential role in determining the molecular growth behavior in the monolayer regime. Stronger molecule–substrate interaction will facilitate amorphous growth. For relatively weaker molecule–substrate interaction, the laterally attractive molecule–molecule interaction will favor island growth at submonolayer stage if diffusion of molecules is not constrained. While the laterally repulsive (weak) intermolecular interaction will usually give rise to 2D liquid-like growth at submonolayer and form ordered structures at monolayer. For example, PTCDA and DM-PBDCI on noble metal surfaces exhibit island growth due to the attractive intermolecular interaction.[51,52] For 1,3,5-triphenylbenzene on Ru(0001), the adsorption energy of the bimolecular system is larger than that of the monomolecular system with DFT calculations, leading to molecular close-packed behavior.[45] However, in the present case, TP molecules on Ru(0001) at low coverage are hardly subject to the ordered structure even if being annealed to higher temperature and only at monolayer can ordered structures occur. Besides, the close-packed domains are more stable than the loosely packed disordering during the scanning (see Fig. 3(a)). Those results suggest TP adsorbed on Ru(0001) conforms to 2D liquid-like growth mode under laterally (weak) repulsive molecule–molecule interaction. As one member of small aromatic molecules, perylene on Cu(100) was also observed to adopt such liquid-like growth mode because of repulsive intermolecular interaction.[53] In the monolayer regime, TP on Au(111) self-assembled into a long-range ordered structure[28] while TP on Ru(0001) formed local ordering. The distinction of electronic structures for Ru(0001) and Au(111) should be the main reason. Some experiments also suggested benzene molecules on Au(111) are still mobile even at high coverage and at low temperature of 4 K[54] while benzene on Ru(0001) can stay immobile and yield a highly ordered overlayer.[55] The d-band center of Au(111) well below the Fermi level causes the bonding of aromatic molecules with Au(111) becoming significantly weaker than that with active transition metal as Ru(0001) with unfilled d bands. The strong π–d interaction between the molecule and the substrate makes weak in-plane van der Waals force between TP molecules subordinated in molecular self-assembly and hence a disordered structure in the long-range distance.

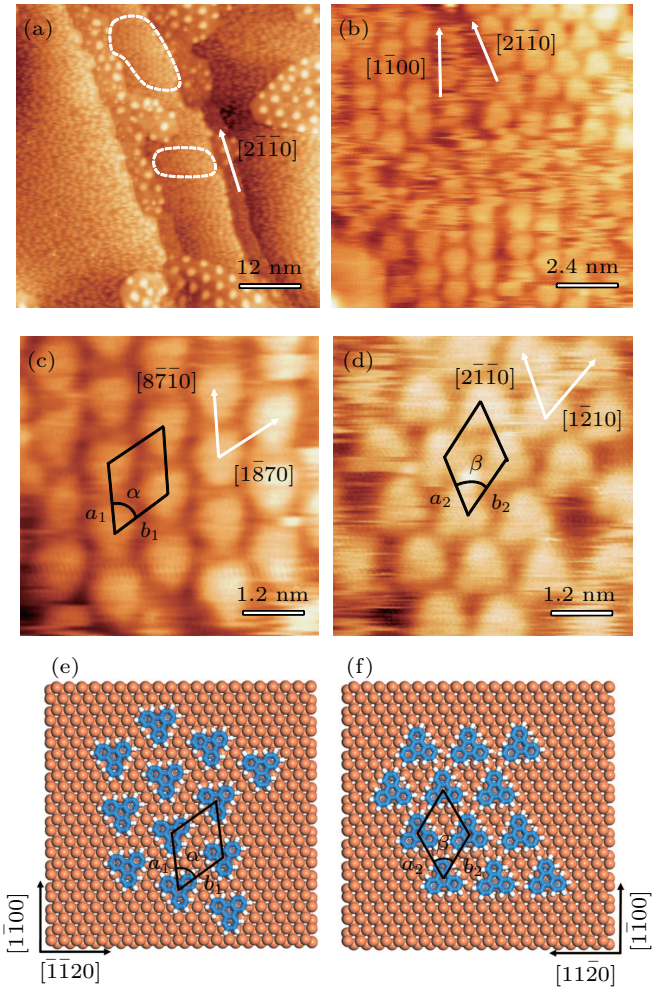


Fig. 3. (a) Overview STM image of ∼ 1.0 ML of TP molecules on the bare Ru(0001) surface covered with partial graphene islands (60 nm×60 nm, $V_{\mathrm{tip}} = -0.141$ V, $I = 0.088$ nA). Small close-packed domains are outlined by white dashed contours. (b) STM image showing coexistence of two close-packed superstructures (12 nm×12 nm, $V_{\mathrm{tip}} = -0.275$ V, $I = 0.101$ nA). (c) The enlarged STM image for close-packed superstructures with the molecular axis nearly going along [$\bar{1}$100]. There is a diminutive rotational angle of 5° or so between the molecular axis and [$\bar{1}$100] direction (6.0 nm×6.0 nm, $V_{\mathrm{tip}} = -0.275$ V, $I = 0.101$ nA). The unit cell is highlighted by the black rhombus. The corresponding structural model is demonstrated in (e). (d) The zoom-in STM image of superstructures with the molecular axis nearly aligned with [1$\bar{1}$00] (6.0 nm×6.0 nm, $V_{\mathrm{tip}} = -0.275$ V, $I = 0.097$ nA). The unit cell is also highlighted by the black rhombus. The corresponding structural model is demonstrated in (f). The blue, gray, and orange hard spheres represent carbon, hydrogen, and Ru atoms, respectively.

4. Conclusions

TP molecules lie flat on the Ru(0001) surface and have a predilection for 2D liquid-like growth mode. They adopt two adsorption configurations with one-to-one ratio of orientational distribution at submonolayer, which are energetically equivalent due to the three-fold symmetries of TP and the substrate. The TP overlayer on Ru(0001) can be converted into graphene nanostructures at 700 K and the grooves formed by graphene islands have confinement effect on the lateral movement of TP molecules due to weak interaction between TP and graphene islands supported by Ru(0001). At TP coverage close to 1.0 ML, two small close-packed domains with a

$(\sqrt{19}\times\sqrt{19})R23.41^\circ$ symmetry and a $p(4\times4)$ symmetry occur. Such a self-assembly behavior of TP on Ru(0001) is the result of the subtle competition between molecule–substrate and molecule–molecule interactions. The strong π–d interaction of TP on the Ru(0001) surface interferes with the formation of a well-defined long-range ordered structure. Our work enlarges the library of small aromatic molecules on active metals and further DFT calculations are needed to understand the adsorption behavior of TP molecules on Ru(0001) in order to control them better for the future electronic devices used for high temperature endurance.

References

[1] Kaneko S, Murai D, Marques Gonzalez S, Nakamura H, Komoto Y, Fujii S, Nishino T, Ikeda K, Tsukagoshi K and Kiguchi M 2016 *J. Am. Chem. Soc.* **138** 1294

[2] Komoto Y, Fujii S, Iwane M and Kiguchi M 2016 *J. Mater. Chem. C* **4** 8842

[3] Trasobares J, Vuillaume D, Theron D and Clement N 2016 *Nat Commun.* **7** 12850

[4] Yan S C, Xie N, Gong H Q, Sun Q, Guo Y, Shan X Y and Lu X H 2012 *Chin. Phys. Lett.* **29** 046803

[5] Li J, Gottardi S, Solianyk L, Moreno Lopez J C and Stohr M 2016 *J. Phys. Chem. C* **120** 18093

[6] DeLoach A S, Conrad B R, Einstein T L and Dougherty D B 2017 *J. Chem. Phys.* **147** 184701

[7] Jeon S, Doak P W, Sumpter B G, Ganesh P and Maksymovych P 2016 *ACS Nano* **10** 7821

[8] Parschau M, Fasel R, Ernst K H, Groning O, Brandenberger L, Schillinger R, Greber T, Seitsonen A P, Wu Y T and Siegel J S 2007 *Angew. Chem. Int. Ed. Engl.* **46** 8258

[9] Abb S, Harnau L, Gutzler R, Rauschenbach S and Kern K 2016 *Nat Commun.* **7** 10335

[10] Otero R, Gallego J M, de Parga A L, Martin N and Miranda R 2011 *Adv. Mater.* **23** 5148

[11] Kumar A, Banerjee K and Liljeroth P 2017 *Nanotechnology* **28** 082001

[12] Jarvinen P, Hamalainen S K, Banerjee K, Hakkinen P, Ijas M, Harju A and Liljeroth P 2013 *Nano Lett.* **13** 3199

[13] Caputo M, Panighel M, Lisi S, *et al.* 2016 *Nano Lett.* **16** 3409

[14] Ashkenasy G, Cahen D, Cohen R, Shanzer A and Vilan A 2002 *Acc. Chem. Res.* **35** 121

[15] Kim J H, Ribierre J C, Yang Y S, Adachi C, Kawai M, Jung J, Fukushima T and Kim Y 2016 *Nat Commun.* **7** 10653

[16] Peyrot D and Silly F 2016 *ACS Nano* **10** 5490

[17] Han Z, Czap G, Chiang C L, Xu C, Wagner P J, Wei X, Zhang Y, Wu R and Ho W 2017 *Science* **358** 206

[18] Ren J, Bao D L, Dong L, Gao L, Wu R, Yan L, Wang A, Yan J, Wang Y, Du S X, Huan Q and Gao H J 2017 *Chin. Phys. B* **26** 086801

[19] Wang H, Sun X, Li D, Zhang X, Chen S, Shao W, Tian Y and Xie Y 2017 *J. Am. Chem. Soc.* **139** 2468

[20] Enache M, Maggini L, Llanes Pallas A, Jung T A, Bonifazi D and Stöhr M 2014 *J. Phys. Chem. C* **118** 15286

[21] Dou R F, Ma X C, Xi L, Yip H L, Wong K Y, Lau W M, Jia J F, Xue Q K, Yang W S, Ma H and Jen A K 2006 *Langmuir* **22** 3049

[22] Xu L, Ding S Y, Liu J, Sun J, Wang W and Zheng Q Y 2016 *Chem. Commun. (Camb)* **52** 4706

[23] Heller L E, Whitleigh J, Roth D F, Oherlein E M, Lucci F R, Kolonko K J and Plass K E 2012 *Langmuir* **28** 14855

[24] Yokoyama T, Yokoyama S, Kamikado T, Okuno Y and Mashiko S 2001 *Nature* **413** 619

[25] Gao H Y, Wagner H, Held P A, Du S, Gao H J, Studer A and Fuchs H 2015 *Appl. Phys. Lett.* **106** 081606

[26] Lin N, Dmitriev A, Weckesser J, Barth J V and Kern K 2002 *Angew. Chem. Int. Ed. Engl.* **41** 4779

[27] Quiñonero D, Frontera A, Deyà P M, Alkorta I and Elguero J 2008 *Chem. Phys. Lett.* **460** 406

[28] Wen R, Yan C J, Yan H J, Pan G B and Wan L J 2011 *Chem. Commun. (Camb)* **47** 6915

[29] Zyss J, Ledoux Rak I, Weiss H C, Bläser D, Boese R, Thallapally P K, Thalladi V R and Desiraju G R 2003 *Chem. Mater.* **15** 3063

[30] Gardner J W 2004 *Electronic Noses & Sensors for the Detection of Explosives* (1st edn.) (Dordrecht: Springer) pp. 29–37

[31] Katsonis N, Marchenko A and Fichou D 2003 *J. Am. Chem. Soc.* **125** 13682

[32] Xu J, Li T, Geng Y, Zhao D, Deng K, Zeng Q and Wang C 2015 *J. Phys. Chem. C* **119** 9227

[33] Kumar S 2004 *Liq. Cryst.* **31** 1037

[34] Turner R J 2015 *Triphenylene as a Scaffold for New Molecular Materials* (Ph.D. Thesis) (Norwich: University of East Anglia)

[35] Gupta M and Pal S K 2016 *Langmuir* **32** 1120

[36] Wyrick J, Kim D H, Sun D, Cheng Z, Lu W, Zhu Y, Berl, K, Kim Y S, Rotenberg E, Luo M, Hyldgaard P, Einstein T L and Bartels L 2011 *Nano Lett.* **11** 2944

[37] Lu B, Zhang H, Li H, Bao S, He P and Hao T 2003 *Phys. Rev. B* **68** 125410

[38] Horcas I, Fernandez R, Gomez Rodriguez J M, Colchero J, Gomez Herrero J and Baro A M 2007 *Rev. Sci. Instrum.* **78** 013705

[39] Cui Y, Fu Q, Zhang H and Bao X 2011 *Chem. Commun. (Camb)* **47** 1470

[40] Gao J F and Ding F 2015 *J. Cluster Sci.* **26** 347

[41] Moritz W, Wang B, Bocquet M L, Brugger T, Greber T, Wintterlin J and Gunther S 2010 *Phys. Rev. Lett.* **104** 136102

[42] Liao Q, Zhang H J, Wu K, Li H Y, Bao S N and He P 2010 *Appl. Surf. Sci.* **257** 82

[43] Feng W, Lei S, Li Q and Zhao A 2011 *J. Phys. Chem. C* **115** 24858

[44] Cai Y, Zhang H, Song J, Zhang Y, Rehman A U and He P 2015 *Nanotechnology* **26** 295601

[45] Song J, Zhang H, Zhang Y, Cai Y, Bao S and He P 2016 *Appl. Surf. Sci.* **367** 424

[46] Wang C S, Bartelt N C, Ragan R and Thurmer K 2018 *Carbon* **129** 537

[47] Zint S, Ebeling D, Ahles S, Wegner H A and Schirmeisen A 2016 *J. Phys. Chem. C* **120** 1615

[48] Weiss K, Gebert S, Wühn M, Wadepohl H and Wöll C 1998 *J. Vac. Sci. Technol. A* **16** 1017

[49] Zhang X, Wang H, Wang S, Shen Y, Yang Y, Deng K, Zhao K, Zeng Q and Wang C 2012 *J. Phys. Chem. C* **117** 307

[50] Rui G, Jialin Z, Songtao Z, Xiaojiang Y, Shu Z, Shuo S, Zhenyu L and Wei C 2017 *Acta Phys. -Chim. Sin.* **33** 627

[51] Glöckler K, Seidel C, Soukopp A, Sokolowski M, Umbach E, Böhringer M, Berndt R and Schneider W D 1998 *Surf. Sci.* **405** 1

[52] Nowakowski R, Seidel C and Fuchs H 2001 *Phys. Rev. B* **63** 195418

[53] Hu F, Zhang H, Mao H, Liao Q and He P 2011 *J. Chem. Phys.* **134** 194702

[54] Mantooth B A, Sykes E C H, Han P, Moore A M, Donhauser Z J, Crespi V H and Weiss P S 2007 *J. Phys. Chem. C* **111** 6167

[55] Witte G and Wöll C 2004 *J. Mater. Res.* **19** 1889